Using modified DNDC biogeochemical model to optimize field management of multi-crop (cotton, wheat, maize) system: a site-scale case study in northern China

Wei Zhang [1], Chunyan Liu [1], Xunhua Zheng [1, 2], Kai Wang [1], Feng Cui [1, a], Rui Wang [1], Siqi Li [1, 2], Zhisheng Yao [1], Jiang Zhu [1]

[1] State Key Laboratory of Atmospheric Boundary Layer Physics and Atmospheric Chemistry, Institute of Atmospheric Physics, Chinese Academy of Sciences, Beijing 100029, P. R. China

[2] College of Earth and Planetary Science, University of Chinese Academy of Sciences, Beijing 100049, P.R. China

[a] Now at the Environmental monitoring station of Jiulongpo district, Chongqing, 630050, P. R. China

Corresponding to: Xunhua Zheng (xunhua.zheng@post.iap.ac.cn)

Abstract It is still a severe challenge to optimize the field management practices for multi-crop system simultaneously aiming at yield sustainability and the minimum negative impacts on climate and qualities of atmosphere and water. This site-scale case study devoted to develop a biogeochemical process model-based approach as a solution to this challenge. The best management practices (BMPs) of a three-crop system growing cotton and winter wheat-summer maize (W-M) in rotation, which is widely adopted in northern China, were identified. The BMPs were referred to the management alternatives with the lowest negative impact potentials (NIPs) among the scenarios satisfying all given constraints. The independent variables to determine the NIPs and those as constrained criteria were simulated by the DeNitrification-DeComposition model modified in this study. Due to the unsatisfactory performance of the model in daily simulations of nitric oxide (NO) emission and net ecosystem exchange of carbon dioxide (NEE), the model was modified to include (i) newly parameterizing the soil moisture effects on NO production during nitrification, and (ii) replacing the original NEE calculation approach with an algorithm based on gross primary production. Validation of the modified model showed statistically meaningful agreements between the simulations and observations in the cotton and W-M fields. Three BMP alternatives with overlapping uncertainties of simulated NIPs were screened from 6000 management scenarios randomly generated by the Latin hypercube sampling. All these BMP alternatives adopted the baseline (currently applied) practices of rotation pattern (3 consecutive years of cotton rotating with 3 years of W-M in each 6-year cycle),

fraction for crop residue incorporation (100%), and deep tillage (30 cm) for cotton. At the same time, these BMP alternatives would use 18% less fertilizer nitrogen and sprinkle or flood-irrigate ~23% less water than the baseline while adopting reduced tillage (5 cm) for W-M. Compared to the baseline practices, these BMP alternatives could simultaneously sustain crop yields, annually enlarge soil organic carbon stock by 4‰ or more, mitigate the aggregate emission of greenhouse gases, NO release, ammonia volatilization, and nitrate leaching by ~7%, ~25%, ~2% and ~43%, respectively, despite ~5% increase in N_2O emission. However, further study is still necessary for field confirmation of these BMP alternatives. Nevertheless, this case study proposed a practical approach to optimize multi-crop system management for simultaneously achieving multiple United Nations Sustainable Development Goals.

1 Introduction

Globally, fiber crops (i.e., cotton) and cereals such as wheat and maize have long played a relevant role in human society because they are primary sources of materials for the textile and food industries. In China, although cotton cultivation only covers 2.0−3.9% of the annual crop harvest area (there was a cotton lint production of 5.3−7.6 million metric tons from 2007−2016), the cultivation of cereals is quite large. Wheat and maize accounted for 39% and 26% of the harvest area and represented 129 and 220 million metric tons of grain, respectively, in 2016 (China Statistical Yearbook, 2017).

Northern China is both the second most important area of cotton production and the largest region of the winter wheat-summer maize double-cropping system (i.e., both crops are harvested within a year, and they are hereinafter referred to as W-M) in the country (e.g., Cui et al., 2014). Crop rotations of cotton and W-M have commonly been grown in this region, alternating every 3−5 years (e.g., Liu et al., 2010, 2014). During the last few decades, the yields of cotton, wheat and maize have been increased by employing intensified agricultural management practices, such as increased fertilizer inputs, advanced irrigation methods and so on (e.g., Han, 2010). A recent study indicated that the cotton cropping system in northern China persistently functioned as an intensive carbon or net aggregate greenhouse gas (GHG) source compared to W-M (Liu et al., 2019). These previous studies have revealed that the change in the storage of soil organic carbon (ΔSOC), net ecosystem aggregate GHG emissions (NEGE) and other biogeochemical processes involving the multiple cropping system in northern China are likely closely related to the rotation pattern of cotton and W-M (e.g., Liu et al., 2010, 2014, 2019; Lv et al., 2014).

To maintain high productivity, the three-crop rotation system for cotton and W-M in northern

China are characterized by large additions of synthetic nitrogen fertilizers and irrigation water (e.g., Chen et al., 2014; Galloway et al., 2004), at 60−140 and 550−600 kg N ha^{-1} yr^{-1}, and 140−200 and 90−690 mm yr^{-1} for cotton and W-M, respectively (e.g., Ju et al., 2009; Liu et al., 2014; Wang et al., 2008). High nitrogen and water inputs can result in high release potentials for nitrogenous pollutants, and they can induce a series of environmental problems, such as increased nitrate (NO_3^-) leaching for water pollution (e.g., Collins et al., 2016). In addition, other field management practices, e.g., tillage and crop residue treatment, can also affect the emissions of reactive nitrogen and contribute to negative environmental effects (e.g., Zhang et al., 2017; Zhao et al., 2016). Therefore, the evaluation of the multiple-cropping system (e.g., rotations of cotton and W-M) is shifting from a single-goal method aimed at increasing crop yields to a multi-goal approach (e.g., Cui et al., 2014; Garnett et al., 2013; Zhang et al., 2018). A multi-goal strategy aims to simultaneously sustain/increase crop productivity to ensure food security, increase SOC content to improve soil fertility, mitigate NEGE to alleviate climate warming, reduce ammonia (NH_3) volatilization and nitric oxide (NO) emission to secure air quality, and abate NO_3^- leaching to protect water quality.

According to the multi-goal approach, an objective method is applied to identify the best management practice (BMP), which evaluates each decision variable with price-based proxies or other measures and screens the best option with the minimal negative impact potential (NIP) under the given constraints at the annual scale (e.g., Cui et al., 2014; Xu et al., 2017). To screen the BMP, it is essential to quantify the biogeochemical effects of management practices at the annual scale. Field experiments are often capable of focusing on only the decision variables of very few management practices during short periods (e.g., Ding et al., 2007; Liu et al., 2010, 2015; Wang et al., 2013a, b). However, this limitation of field experiments can be overcome potentially by process-oriented biogeochemical models, such as DeNitrification-DeComposition (DNDC) (Li et al., 1992; Li, 2000, 2007, 2016), DAYCENT (Delgrosso et al., 2005), and LandscapeDNDC (Haas et al., 2012).

A three-crop (cotton, winter wheat and summer maize) system in southern Shanxi Province was selected for this model-based site scale case study. This study was to (i) diagnose problems of DNDC95 model version that has been validated in Cui et al. (2014) against the comprehensive field measurements of the selected W-M fields, (ii) make modifications and then validate the modified

model for both cotton and W-M cropping systems, especially for the variables to determine NIPs and those involved in given constraints; and (iii) investigate the biogeochemical effects of various rotation patterns with different field management practices, and then, identify the multi-goal BMP alternatives based on the modified model simulations. These efforts were undertaken to test two hypotheses. One is that a validated process-oriented biogeochemical model is capable of addressing a challenging issue – optimization the field management practices of a three-crop rotation system. The other hypothesizes that the field managements of an intensive three-crop rotation system can be optimized to simultaneously sustain the current crop yields, annually increase 4‰ of the SOC stock so as to implement the International "4 Per 1000" Initiative (https://www.4p1000.org/) – an action to the Paris Agreement on combating climate change, mitigate aggregate greenhouse gas emission and reduce other negative impacts on the environment.

2 Materials and methods

2.1 Brief introduction to DNDC95

The original DNDC95 model used by Cui et al. (2014) and in this study is one of the latest DNDC versions (www.dndc.sr.unh.edu/model/GuideDNDC95.pdf). This model consists of two components with six modules in total. Driven by the given primary ecological factors, the former component simulates the field states of a soil-plant system, such as the soil chemical and physical status, vegetation growth and organic matter decomposition. Driven by the soil-regulating variables yielded by the former component, the latter component simulates the core biogeochemical processes of carbon and nitrogen transformations and the physical processes of liquid and gas transportations and thus the annual dynamics of net ecosystem exchanges of carbon dioxide (CO_2) (NEE); emissions of methane (CH_4), nitrous oxide (N_2O), NH_3 and NO; and NO_3^- leaching and the inter-annual dynamics of SOC and NEGE. These features enable the model to investigate the integrative biogeochemical effects of the rotation patterns of multiple crops and/or other management practices based on comprehensive validation. The minimum inputs used to facilitate the model simulation include (i) the meteorological variables of daily precipitation and maximum/minimum temperature; (ii) the soil (cultivated horizon) properties of the clay fraction, bulk density, SOC content and pH; (iii) the crop parameters for the yield potential, thermal degree days (TDD) for maturity, and the mass fractions and carbon-to-nitrogen (C/N) ratios of the grain, root and leaf plus stem; (iv) the management practice variables of sowing and

harvest (dates), fraction of incorporated/retained residue at harvest, tillage (date and depth), irrigation (date, method and water amount), and fertilization (date, type, method, nitrogen amount and C/N ratio of organic manure); and (v) other variables (annual means of the NH_3 concentration in the atmosphere and the ammonium plus NO_3^- concentration in rain water). For more details about the model, please see Li et al. (1992) and Li (2000, 2007, 2016).

2.2 Problem diagnosis and model modification

The daily simulations of the original DNDC95 showed poor model performance for NO emissions from the cotton field, e.g., with a very negative Nash-Sutcliffe efficiency index (NSI) of –1.03 for the 333 observations in 2009. Meanwhile, the original model often failed to capture the daily high NEE fluxes on rainy or cloudy days despite the agreement between the simulation and observation of the annual cumulative NEE (Cui et al., 2014). According to the program codes, a constant fraction (0.003) of a nitrification rate (F_n, in g N m^{-2} d^{-1}) was adopted in the original model to calculate the daily NO production in the nitrification process. This was found to account for the former problem as the fraction could vary with soil moisture, mechanically similar with the N_2O production in nitrification (shown by the model program codes). The later problem was ascribed to the adopted algorithm to calculate daily NEE. In the original model, a daily NEE flux was calculated as the residue of daily CO_2 release by soil heterotrophic respiration and daily CO_2 uptake by the increase in cumulative net primary production (NPP). The daily cumulative NPP was calculated by portioning the input of potential crop yields to the day following a given NPP growth curve (shown by the model program codes; Li, 2016). Consequently, the insensitivity of a daily NPP increase to radiation intensity reduction resulted in a more negative daily NEE on a rainy or cloudy day. The model was modified in this study, as follows, to solve these two problems.

In the model version modified in this study, the effect of the soil moisture (SM) in water-filled pore space (WFPS, dimensionless 0−1 fraction) on NO production was parameterized by referring to that for N_2O production during nitrification and incorporated into the function by replacing the constant fraction mentioned above (Eq. 1). This modification was adopted to reflect that high soil moisture facilitates the production of NO as a by-product in nitrification (NO_p, in g N m^{-2} d^{-1}). The maximum fraction of NO production (K_n, dimensionless 0−1 fraction) during nitrification was calibrated as 0.03 using the observed daily NO fluxes from October 2007 to October 2008. The other observations of

145 daily and annual NO fluxes from both adjacent lands with different field treatments (Table S1) were
146 used to validate this modification.

$$NO_p = \quad SM^{5.0} K_n F_n \tag{1}$$

147 In the model version modified in this study, a daily NEE flux (g C m^{-2} d^{-1}) is calculated as the
148 residue of the daily CO_2 release from ecosystem respiration (ER, in g C m^{-2} d^{-1}) and daily CO_2 uptake
149 due to gross primary production (GPP, in g C m^{-2} d^{-1}). While the daily ER is simulated as it is in the
150 original model, the daily GPP is calculated using Eq. 2 that is a widely applied hyperbola function of
151 photosynthetically active radiation (PAR, in mmol m^{-2} d^{-1}) (e.g., Wang et al., 2013a; Zheng et al.,
152 2008).

$$GPP = \alpha PAR\ GPP_{max} / (\alpha PAR + GPP_{max}) \tag{2}$$

153 The photosynthetic parameters in Eq. 2, α (g C $mmol^{-1}$) and GPP_{max} (g C m^{-2} d^{-1}), denote
154 apparent quantum yield and maximum GPP, respectively. Each parameter is quantified as the product
155 of shoot standing biomass (B_s, in g C m^{-2}) and biomass-specific apparent quantum yield (f_1, in g C
156 $mmol^{-1}$ (g C m^{-2})$^{-1}$) or specific GPP_{max} (f_2, in g C m^{-2} d^{-1} (g C m^{-2})$^{-1}$) corrected by an adaptation factor
157 (a, dimensionless) reflecting inter-annual variations of a crop (Eqs. 3−4). The variable B_s is simulated
158 as it is in the original model. The seasonal dynamics of f_1 and f_2 is a function of normalized plant
159 developing stage (ds, dimensionless 0−1 fraction) (Eqs. 5−6). The functions of f_1 and f_2 take the forms
160 presented by Zheng et al. (2008) for winter wheat while their empirical parameters of a, b, c, d_1, d_2, g, h,
161 i, j, l and m, can be calibrated to adapt both functions to given conditions. Two daily NEE fluxes per
162 week were randomly selected from the year-round eddy covariance observations in both cotton and
163 W-M cropping systems (Cui et al., 2014; Liu et al., 2019; Wang et al., 2013a) to calibrate the values of
164 these parameters specifically for cotton, winter wheat and summer maize, while remaining daily data
165 (independent NEE observations) were used to evaluate this modified NEE algorithm. For the calibrated
166 values of these parameters, refer to Table S2.

$$\alpha = a f_1 B_s \tag{3}$$

$$GPP_{max} = a f_2 B_s \tag{4}$$

$$f_1(ds) = b e^{-cds} \ (ds \geq d_1) \tag{5}$$

$$f_1(ds) = ge^{hds} \ (ds < d_1)$$
$$f_2(ds) = ie^{-jds} \ (ds \geq d_2)$$
$$f_2(ds) = lds + m \ (ds < d_2) \quad (6)$$

2.3 Brief introduction to the selected field site and information of the data for model evaluation

The field site (34°55.50′N, 110°42.59′E and altitude of 348 m) selected for this modeling case study is located at Dongcun Farm, near Yongji County, Shanxi Province, in northern China. The site is subject to a temperate continental monsoon climate, and it had an annual precipitation of 580 mm and a mean air temperature of 14.4 °C from 1986−2010 (Cui et al., 2014). Cotton, winter wheat and summer maize are the major crops grown at this farm and the surrounding regions. Field experiments were performed on two adjacent lands (each of which was 100 m wide and 200 long) for cotton and W-M in 2007−2010. The soil of the land cultivated with cotton and W-M was clay loam, with approximately 38% and 32% clay (< 0.002 mm), 57% and 50% silt (0.002−0.05 mm), 5% and 18% sand (0.05−2 mm), 10.0 and 11.3 g kg^{-1} SOC, 1.1 and 1.1 g kg^{-1} total nitrogen and pH (in H_2O) of 8.0 and 8.7 at a 0−10 cm depth and bulk densities (0−6 cm depth) of 1.20 and 1.17 g cm^{-3}, respectively (Liu et al., 2010, 2011, 2012). A sprinkler system was applied to both lands. For more detailed information on the field experiments and observed data, please refer to Cui et al. (2014), Liu et al. (2010, 2011, 2014, 2015) and Wang et al. (2013a, b).

The modified model was validated with observations in both lands. The daily meteorological data from 2004−2010 were obtained directly from Cui et al. (2014). The measured data were used directly for the minimum required soil properties. The input data on the field capacity and wilting point in WFPS were 0.65 and 0.2, respectively (Cui et al., 2014). The crop parameters for cotton were directly determined by the field measurements, which were 1900 kg C ha^{-1} for potential grain yield (1.2 times the mean of the measured values), 0.41 and 25, 0.16 and 40, and 0.43 and 40 for the mass fractions and C/N ratios of the grain, root and leaf plus stem, respectively, and 3600 °C for the TDD. Detailed management practices (Table S3) were obtained from Li et al. (2009) and Liu et al. (2014). Different from the locally conventional fertilizer application rate of 110−140 kg N ha^{-1} yr^{-1} for cotton, the fertilizer doses for the experimental cotton field in 2007 and 2008 were reduced to 66−75 kg N ha^{-1} yr^{-1} to avoid the overgrowth of the leaves in place of seeds or lint. The data of the cotton field available for the model calibration and validation included the daily observed soil (5 cm depth) temperature,

topsoil (0−6 cm) moisture, daily NEE from eddy covariance measurement from 2008 to 2009, sub-weekly observed CH_4 fluxes in the growing season of 2010 (Liu et al., 2010, 2014, 2019; Wang et al., 2013b), daily N_2O and NO fluxes from 2007 to 2008, annually measured grain yields from 2008 to 2010, and annually NO_3^- leaching from 2008 to 2009. All the data used by Cui et al. (2014) in validation of the original model were used to re-validate the modified model performances for the selected W-M fields with different field managements. In addition, two observations of the cumulative NH_3 volatilizations following urea topdressing to the winter wheat in the spring of 2008 (Tong et al., 2009) were also involved in evaluation of the model performance (Yang et al., 2011). The information for all the data used in the modified model calibration and validation are detailed in Table S1.

2.4 Scenario settings and simulations

For the investigated three-crop system, this study attempted to identify the BMP alternatives with the best rotation pattern between cotton and W-M and the optimized field management practices of this rotation pattern. For this purpose, six rotation pattern scenarios (hereinafter referred to as R_0, R_1, ..., R_5) were set for a 6-year cycle that was widely applied by the local farmers (Liu et al., 2010, 2011, 2014). The subscript number of each rotation pattern represents the number of the consecutive years with cotton cultivation. For instance, R_0 denotes a 6-year monoculture of W-M, and R_2 the rotation pattern with 2-year continuous cotton rotated with 4-year of continuous W-M. Because the local farmers typically did not adopt cotton monoculture for longer than five years, the longest cotton monoculture lasted for only 5 years (R_5). The transitions between cotton and W-M in the scenario rotations are detailed in Table S4.

As for the setting of the field management scenarios for the individual rotation patterns, four field management factors were considered, which were (i) nitrogen fertilizer dose, (ii) water amount (iii) method of irrigation, and (iv) depth of tillage. The values of these factors used for the baseline scenario were known as the observations for the conventional management practices in the experimental region (Tables S3, S4 and S5). The nitrogen doses of the baseline were 110 and 430 kg N ha^{-1} yr^{-1} for the cotton and W-M, respectively. Over the last few decades, the fields in this region have been mostly flood-irrigated (Liu et al., 2010). Thus, flood-irrigation was chosen as the baseline method. The baseline timings and water amounts were established by referring to the 10- to 30-d cumulative precipitation prior to the individual irrigation events and the recorded timings and water amounts of the

conventional management practices in the two adjacent lands. Thus, the irrigation frequencies and annual cumulative water amounts of the baseline varied from 1 to 3 times and 75 to 230 mm yr^{-1} for cotton and 4 to 6 times and 290 to 510 mm yr^{-1} for W-M (Table S5). The fraction of 100% for residue incorporation and the conventional tillage to a depth of 20 for W-M and 30 cm for cotton were applied for the baseline practices. To screen the BMPs by fully taking into account the independent and interactive effects of rotation patterns and field management on the NIPs, totally 6000 field management scenarios (each being a combination of the four management factors) for all the six rotation pattern scenarios (1000 for each) were randomly generated. The fertilizer doses and irrigation water amounts were randomly selected within their lower and upper bounds of continuous variations, using the Latin hypercube sampling. The lower and upper bounds for nitrogen fertilizer doses (44−172 and 110−430 kg N ha^{-1} yr^{-1}) and irrigation water amount (40−100 mm per event) were set as 40% and 100% of the baseline, respectively. Only two irrigation methods, flooding (IF) as the baseline and sprinkling (IS), were included for the random sampling of this management factor. For cotton, the tillage depth was fixed at 30 cm. For W-M, four tillage depths (0 cm for no-till, 5 and 10 cm for reduced tillage, and 20 cm for the conventional practice) were included for random sampling of this factor. The BMPs for each rotation pattern scenario were first screened from 1000 field management scenarios. Then, the BMP alternatives were finally screened from these BMPs of the individual rotation pattern scenarios. These identified BMP alternatives would include the scenarios with overlapping uncertainties of NIPs, for which the random error at one times standard deviation (SD, instead of two times SD) for the total simulation error was adopted for the NIP of each scenario so as to achieve a relatively high screening precision. The decision variables and NIP of baseline management scenarios for each rotation pattern scenario were used to particularly address the biogeochemical effects of rotation pattern.

An 18-year simulation was performed for each scenario. The annual averages for the simulated yields, decision variables and NIPs were used to address the biogeochemical effects of rotation patterns or to screen the BMP alternatives. The simulations of all scenarios were driven by the meteorological data observed at the Yuncheng station (approximately 60 km east to the experimental site) from 1996−2013 (http://data.cma.cn/data/cdcindex/cid/6d1b5efbdcbf9a58.html). To stabilize the carbon and

nitrogen dynamics and reduce the residual effects of the initial conditions (Palosuo et al., 2012; Zhang et al., 2015), a 12-year spin-up for each scenario was performed (i.e., a period of two consecutive 6-year rotation cycles) before the 18-year simulation. The spin-up for each scenario was driven by the same rotation pattern and field management practices as this scenario.

2.5 Method for identifying the best management practices

An objective method jointly relying on three constraints and NIPs was adopted in this study to screen the BMPs from given scenarios. These constraints included (i) stable or increased crop yields, (ii) annually increased SOC stock by 4‰ or more, and (iii) reduced NEGE by 5% or more. In the present study, the NEGE was determined by summing up the emissions of CH_4 and N_2O and $-\Delta SOC$, which was quantified as a CO_2 equivalent (CO_2eq) quantity. In the quantification of a NEGE, the global warming potentials at 100-year time horizon, 34 for CH_4 and 298 for N_2O (IPCC, 2013), were used to convert the quantities of both gases into CO_2 equivalents. A NIP was expressed as a price-based proxy quantity in US\$ ha^{-1} yr^{-1} and used to evaluate the potential for a climatically and environmentally integrative impact exerted by a set of field management practices for multi-crop system. The NIP was determined as a linear function of the individual decision variables, following Eq. 7, wherein the multi-goal decision variables, NEGE, NH_3, NO, N_2O_{ODM}, and NL, represent the annual net ecosystem aggregate GHG emission (Mg CO_2eq ha^{-1} yr^{-1}), NH_3 volatilization, NO emission, release of N_2O as an ozone layer depletion matter, and hydrological nitrogen loss (mainly by NO_3^- leaching), respectively (kg N ha^{-1} yr^{-1} for all the nitrogen-based variables). The coefficients k_1, k_2, k_3, k_4 and k_5 are mass-scaled price-based proxies for the NEGE, NH_3, NO, N_2O_{ODM}, and NL, with values of 7.00 US\$ Mg^{-1} CO_2eq and 5.02, 25.78, 1.33 and 1.92 US\$ kg^{-1} N, respectively (Cui et al., 2014). A lower NIP indicated a better set of management practices that can exert smaller negative impacts on the climate and environment. Accordingly, the BMP was identified as the scenario with the lowest NIP among the scenarios that could satisfy all three constraints.

$$NIP = k_1NEGE + k_2NH_3 + k_3NO + k_4N_2O_{ODM} + k_5NL \quad (7)$$

2.6 Method for uncertainty quantification

The model simulation error (ε_s) of a NIP, a constraint variable (e.g., crop yield) or a decision variable involved in Eq. 7 represented the total simulation uncertainty. It was made of two components. One was the input-induced uncertainty (ε_{input}) due to the uncertainties of input items; and the other was

the model uncertainty (ε_{model}) due to insufficiencies in scientific structure or process parameters.

The ε_{input} of a simulated variable was a random error if the uncertainties of model input items were known as random errors. It was estimated using the Monte Carlo test with the Latin hypercube sampling within the uncertain ranges (95% confidence interval (CI)) of sensitive input items. In DNDC, the four basic soil properties (bulk density, pH, clay fraction and SOC content) as input items were sensitive to the model outputs (e.g., Li, 2016). Accordingly, the uncertainties of these soil properties were regarded to be the major dominators for the uncertainties of the model outputs, such as the constraint/decision variables, or NIP. The initial bulk density, pH, clay fraction and SOC content ranged 1.13−1.25 g cm^{-3}, 8−8.7, 0.31−0.39 and 9−12 g kg^{-1} (at the 95% CI), respectively, which were adapted from the means and two times SD of spatially replicated observations in the two adjacent lands (Liu et al., 2014, 2019). A uniform distribution for each of these soil properties was assumed in Monte Carlo test, in which the sampling and simulation were iterated until the mean of simulated NIPs for all iterations converged to a certain level within a tolerance of 1%. The NIP uncertainty due to the model input uncertainties was presented as the SD of these iterated simulations.

An ε_s was systematic error reflecting a model simulation bias diverging from the truth. In this regard, the ε_s of a constraint/decision variable could be estimated using the slope of a zero-intercept univariate linear regression of simulations against observations ($ZIR_{s\text{-}o}$) or model relative biases (MRBs) resulted from model validation (Eq. 8). The MRBs were used only in case a significant $ZIR_{s\text{-}o}$ was failed to be obtained in model validation. To ensure a relatively high BMP screening precision, the random uncertainty of the ε_s of a NIP was presented as one times SD, instead of the two times SD to represent 95% CI, as the BMP alternatives were referred to the management scenarios with overlapping NIP uncertainties. For a constraint/decision variable, the mean or SD of ε_s in an absolute magnitude was estimated as the product of (i) an adjusting factor, (ii) the simulated variable quantity, and (iii) an error factor. The adjusting factor was obtained from model validation, which was estimated as the mean of the ratios of individual observations to simulations. The error factor for a variable with a significant $ZIR_{s\text{-}o}$ was given as (Mean-$Slope_{s\text{-}o}$−1) ± SD-$slope_{s\text{-}o}$, wherein Mean-$Slope_{s\text{-}o}$ and SD-$slope_{s\text{-}o}$ denote the mean and SD of the $ZIR_{s\text{-}o}$ slope, respectively. The item prior to and following the "±" was used to estimate the mean and SD of the ε_s. For a variable failed to obtain a significant $ZIR_{s\text{-}o}$ in model

validation, the mean and SD of the error factors were given as the mean and SD of the MRBs. The mean of the ε_s for a NIP was estimated by simply summing up the weighted absolute ε_s of individual decision variables. This was because the decision variables involved in the additive items of Eq. 7 were independent from each other. Meanwhile, the SD of the ε_s for a NIP was mathematically propagated from the SDs of the absolute ε_s of the decision variables.

In this study, the constraint variables included crop yield, $-\Delta$SOC and NEGE while NEGE was also one of the decision variables. Although there was no direct measurement of $-\Delta$SOC and NEGE, their observation-oriented estimates were involved in the model validation, which provided the basis for the ε_s estimation of either variable. For the experimental fields with NEE observations, there was no significant input quantity of organic matter in manure or any other form while crop residues were fully incorporated into the soil. In these cases, each annual/seasonal $-\Delta$SOC could be estimated as the sum of annual/seasonal NEE and yields, according to the mass conservation law, and used to represent the observation, with its uncertainty propagated from the random errors of the annual/seasonal yield and NEE measurements. The random error of this observation-oriented $-\Delta$SOC that represented the annual/seasonal net CO_2 emission from the cropping system and those of the observed annual cumulative CH_4 and N_2O were propagated to estimate the observational error of the annual/seasonal NEGE. These observation-oriented estimates of $-\Delta$SOC or NEGE were involved in model validation.

2.7 Statistics and analysis

Statistical criteria simultaneously used to evaluate the model validity included (i) the index of agreement (IA) (Eq. 9), (ii) the NSI (Eq. 10) (e.g., Moriasi et al., 2007; Nash and Sutcliffe, 1970), (iii) the determination coefficient (R^2) (Eq. 11) and slope of a ZIR of observations against simulations (Jiang, 2010; Li et al., 2019), and (iv) the MRB (Eq. 8) (e.g., Congreves et al., 2016; Willmott and Matsuura, 2005). In Eqs. (8−11), k and n (k = 1, 2..., n) denote the kth pair and the total pair number of the values, respectively, and $\bar{o}$ represents the mean of the observations (o), respectively, and $\hat{o}$ is the predictions using the ZIR. The IA index fell between 0 and 1, with a value closer to 1 indicating a better simulation, and vice versa. An NSI value between 0 and 1 indicated acceptable model performance. Better model performance was indicated by a slope and an R^2 value those were closer to 1, and vice versa. An |MRB| value smaller than the double coefficients of variation (CVs) of replicated observations implicated a valid simulation (Dubache et al., 2019).

$$\mathrm{MRB} = \frac{s_k}{o_k} - 1 \quad (8)$$

$$\mathrm{IA} = 1 - \frac{\sum_{k=1}^{n}(s_k - o_k)^2}{\sum_{k=1}^{n}(|s_k - \bar{o}| + |o_k - \bar{o}|)^2} \quad (9)$$

$$\mathrm{NSI} = 1 - \frac{\sum_{k=1}^{n}(o_k - s_k)^2}{\sum_{k=1}^{n}(o_k - \bar{o})^2} \quad (10)$$

$$R^2 = 1 - \frac{\sum_{k=1}^{n}(o_k - \hat{o}_k)^2}{\sum_{k=1}^{n}(o_k - \bar{o})^2} \quad (11)$$

In this study, the statistical analysis and graphical comparison were performed with the SPSS Statistics Client 19.0 (SPSS Inc., Chicago, USA) and Origin 8.0 (OriginLab, Northampton, MA, USA) software packages.

3 Results

3.1 Validation of daily simulations for both cropping systems

The seasonal dynamics and magnitudes of the soil (5 cm) temperature and topsoil (0−6 cm) moisture were predicted well by the model simulations (Figs. 1a−b). The sound model performance was indicated by the IA, NSI, and ZIR slope and R^2 values of 0.98 and 0.83, 0.93 and 0.15, 0.93 and 0.83, and 0.95 (n = 677, p < 0.001) and 0.42 (n = 432, p < 0.001) for the temperature and moisture, respectively.

As compared to the original model, the modified model showed much better performances in simulating daily NEE fluxes from both cropping systems. It particularly well simulated the abrupt NEE fluxes on cloudy or rainy days in the growing season (Figs. 1c−e). In comparison with the original model for daily NEE simulations, the modified model enhanced the IA, NSI, and ZIR slope and R^2 from 0.74 to 0.81, 0.32 to 0.60, 0.60 to 0.96 and 0.27 to 0.60 (n = 261, p < 0.001), respectively, for the cotton field, and from 0.75 to 0.80, 0.30 to 0.51, 0.69 to 0.80 and 0.45 to 0.55 (n = 311, p < 0.001), respectively, for the W-M field. For the CH_4 uptake, the observations and simulations showed similar seasonal variations (Fig. 1f), with the IA, NSI and ZIR slope and R^2 of 0.68, < 0, 0.70 and 0.08 (n = 69, p = 0.018), respectively.

The simulated seasonal patterns and peak emissions of N_2O and NO generally matched the observations (exemplified by Figs. 1g−h for the cotton field). In comparison with the original model for daily N_2O flux simulations, the modified model performed comparably well for the cotton field, with NSI of around −0.45, ZIR slope ~0.49 and R^2 of ~0.39 (n = 592, p < 0.001), while it showed better performance for the W-M fields, with IA, NSI and ZIR slope and R^2 of 0.69 versus 0.52, 0.03 versus

−0.26, 0.62 versus 0.46 and 0.16 (n = 976, p < 0.001) versus "not available", respectively. Relative to original model, the modified model showed improved simulations for the daily NO fluxes from the cotton field, with increased IA, NSI, and ZIR slope and R^2 from 0.62 to 0.78, −1.03 to −0.04, 0.37 to 0.54 and 0.09 to 0.39 (n = 333, p < 0.001), respectively, while it performed comparably well for those from the W-M fields, with IA, NSI, and ZIR slope and R^2 of ~0.82, ~0.32, ~0.74 and 0.35−0.40 (n = 967, p < 0.001), respectively.

In comparison with the observed daily NH_3 fluxes (measured using micrometeorological technique) following single fertilization event of the maize season in 2008, the modified model simulations showed IA, NSI, and ZIR slope and R^2 of 0.87, 0.12, 0.68 and 0.53 (n = 11, p = 0.07), respectively. However, the model failed to capture the immediate responses of daily NH_3 fluxes to the urea addition to the wheat fields, which were measured using a quasi-dynamic chamber method.

3.2 Validation of simulated variables in annual/seasonal cumulative quantities

For the cotton yields (seeds plus lint) over the three consecutive experimental years (2008−2010), the simulations were consistent with the observations in terms of the smaller |MRBs| (0.4−24%) than the double CVs (39−56%) of the spatially replicated measurements. For all the experimental treatments of the cotton, wheat and maize, the simulated yields of both the modified and original model highly agreed with observations (Fig. 2a), with IA of 0.93−0.95, NSI of 0.75, and ZIR slope and R^2 of 0.96−1.00 and 0.75−0.78, respectively (n = 35, p < 0.001). This validation resulted in an adjusting factors of 0.96 and smaller error factors of 3.0 ±1.6% for crop yields simulated by the modified model.

For the annual cumulative NEE of the cotton field during the two consecutive year-round periods and the seasonal cumulative NEE in two wheat seasons and one maize season, the simulations of both model versions showed comparably significant agreements with the observations (Fig. 2b), with IA of 0.99−1.00, NSI of 0.95−1.00, and ZIR slope and R^2 of 0.92−1.02 and 0.97−0.99, respectively (n = 5, p ≤0.000−0.002). The modified model simulations showed |MRBs| of 6−16%, which were much less than the reported CV (25%) of the eddy covariance observations.

As compared to the annual/seasonal NEGE quantities derived from the observations of crop yields, annual/seasonal cumulative NEE and fluxes of CH_4 and N_2O, the simulations implicated good performance of the modified model (Fig. 2c), with IA of 0.96, NSI of 0.77, ZIR slope and R^2 of 0.73 and 0.91 (n = 5, p = 0.013). Although the simulations showed an average overestimation of ~25%, their

|MRBs| were only 17−72% (33% on average) of the observation-oriented CVs (27−170%, with a mean of 91%), implicating a statistically meaningful good performance of the modified model. This validation resulted in an adjusting factor of 0.73 and error factors of 25 ± 19% for the annual/seasonal NEGE simulated by the modified model.

In comparison with the annual/seasonal ΔSOC quantities estimated from the observed crop yields and annual/seasonal cumulative NEE, the simulations by the modified model (Fig. 2d) showed IA of 0.96, NSI of 0.75, and ZIR slope and R^2 of 0.71 and 0.92 (n = 5, p = 0.011). The ZIR slope indicated an average overestimation of the model by ~30%. Nevertheless, the |MRBs| of the individual simulations were only 4−79% (30% on average) of the observation-oriented CVs (30−210%, with a mean of 97%), still indicating a statistically meaningful consistence. This validation resulted in an adjusting factor of 0.71 and error factors of 30 ± 19% for the annual/seasonal ΔSOC simulated by the modified model.

The model simulations of the annual cumulative CH_4 uptake in 2009 and 2010 showed significant agreements (Fig. 2e), with IA of 0.98, NSI of 0.91, and ZIR slope and R^2 of 1.00 and 0.91 (n = 7, p < 0.001). The |MRBs| were only 5−56% (25% on average) of the double CVs (10−24%, with a mean of 17%) for the spatially replicated observations. This validation resulted in an adjusting factor of 1.00 and error factors of −0.2 ± 1.7% for the modified model simulations of cumulative CH_4 uptake.

The modified model simulations of the annual cumulative N_2O emissions from all the field experimental treatments of the cotton and W-M fields were comparable with the observations (Fig. 2f), showing IA of 0.94, NSI of 0.72, and ZIR slope and R^2 of 0.90 and 0.83 (n = 12, p < 0.001). The |MRBs| of the individual simulations were only 6−93% (36% on average) of the double CVs (23−64%, with a mean of 47%) for the spatially replicated observations. For the annual cumulative N_2O emissions simulated by the modified model, this validation resulted in an adjusting factor of 0.90 and error factors of 8.7 ± 4.5%.

As compared to annual cumulative N_2O emissions, slightly better consistence with observations was obtained for the modified model simulations of the annual cumulative NO emissions from the cotton and W-M fields under different experimental conditions (Figs. 2f−g). The NO simulation showed IA of 0.97, NSI of 0.85, and ZIR slope and R^2 of 0.90 and 0.94 (n = 11, p < 0.001). The |MRBs| of the individual simulations were only 2−52% (23% on average) of the double CVs (30−99%, with a

mean of 66%) for the spatially replicated observations. This validation provided an adjusting factor of 0.90 and error factors of 10.1 ± 3.2% for the cumulative NO emissions simulated by the modified model.

The simulations of the cumulative NH_3 volatilizations during the 11 days following the three urea application events, with one in the maize field in summer and two in the winter wheat fields (with flood-irrigation and sprinkling, respectively) in spring (Fig. 2h), showed IA of 0.97, NSI of 0.86, and ZIR slope and R^2 of 1.00 and 0.86 (n = 3, p = 0.246). The simulations resulted in smaller |MRSs| (3.8−8.8%, −0.4% on average) than the double CVs (16−18%) for the spatially replicated measurements, despite the model failure in capture the quick responses of daily NH_3 fluxes to the urea top-dressing events. This validation resulted in an adjusting factor of 1.00 and error factors of −0.4 ± 7.3% for the modified model simulations of cumulative NH_3 volatilization following nitrogen applications.

The modified model simulations of the cumulative NO_3^- leaching from cotton field in two consecutive years agreed with the observations, in terms of the smaller MRBs of −32% to −27% than the two times CVs (109−115%) for the spatially replicated observations. These MRBs represented the model-underestimations by respectively 3−4 and 13−21 kg N ha^{-1} yr^{-1} for the annual NO_3^- leaching rates in the cotton and W-M fields subject to the currently applied field management practices. This validation derived an adjusting factor of 1.42 and error factors of −29 ± 4% for the modified model simulations.

The above results suggested that the modified DNDC95 model was especially applicable at this field site for investigating the biogeochemical effects of different rotation patterns between the cotton and W-M and those exerted by different management practices, and thus was capable of BMP identification.

3.3 Biogeochemical effects of different cotton and wheat-maize rotation patterns

Figure 3 illustrated the dynamics of the crop yields and each decision variable resulting from the consecutive simulations over 18 years for all the rotation patterns subject to the field management practices of the baseline scenario. Figure 4 showed the relationship between the annual average of each decision variable and the number of consecutive years of cotton monoculture within the rotation patterns.

The average grain yields for the cotton, wheat and maize were not significantly different among

445 the various rotation patterns, with averages of 3.5, 4.8 and 6.7 kg dry matter ha^{-1} for cotton, wheat and
446 maize, respectively (Figs. 3a−c).

447 For the dynamic changes in the annual SOC stocks, the values were generally positive for the
448 W-M but negative for the cotton, except for the first year after the transition to this fiber crop. As
449 indicated by Fig. 3d, the simulated SOC contents over the 18-year period increased for R_0, R_1, R_2 and
450 R_3 but decreased for R_4 and R_5. The annual average $-\Delta$SOC increased significantly ($p < 0.001$) with an
451 increase in the consecutive years of cotton monoculture from 0 to 5 within the 6-year rotation cycle
452 (Fig. 4a). The rotation patterns with the baseline management showed small variations in the CH_4
453 uptake (Fig. 3e), with the uptake rates ranging from 1.6 to 2.1 kg C ha^{-1} yr^{-1}. However, the annual
454 averages for the CH_4 uptake increased significantly ($p < 0.001$) with the increased consecutive years of
455 cotton monoculture (Fig. 4b). For N_2O, the annual emissions showed large inter-annual variations (Fig.
456 3f), with CVs of 26−48%. In addition, the average emissions of this gas decreased significantly from
457 4.6 to 2.6 kg N ha^{-1} yr^{-1} (Fig. 4c) after increasing consecutive years of cotton monoculture ($p < 0.001$).
458 As a result, the NEGE was significantly promoted ($p = 0.002$) (Figs. 3g and 4d).

459 Regarding the gaseous air pollutants NH_3 and NO, the simulated emissions ranged from 17 to 103
460 and 0.5 to 3.3 kg N ha^{-1} yr^{-1}, respectively (Figs. 3h−i). Figures 4e and f showed that the average annual
461 emissions of both gases were significantly reduced after increasing the consecutive years of cotton
462 monoculture ($p \leq 0.001$). The annual NO_3^- leaching of the different rotation patterns displayed
463 significant inter-annual variations (Fig. 3j), with CVs of 41−69%. Thus, the annual averages for NO_3^-
464 leaching changed insignificantly in response to the consecutive years of cotton monoculture ($p < 0.056$;
465 Fig. 4g).

466 The NIP varied significantly among the various rotation patterns ($p < 0.001$), declining from 610
467 to 324 US$ ha^{-1} yr^{-1} with increased consecutive years of cotton monoculture (Fig. 4h). For the three
468 constraints, the crop yields showed no obvious differences among the various rotation patterns. Both R_0
469 and R_5 represented the typical rotation patterns in the region. The simulations for the former indicated
470 the greatest increase in SOC and the lowest NEGE but the highest NIP, while those for the latter
471 showed the greatest SOC loss and the largest NEGE but the lowest NIP (Figs. 4a, d and h). These
472 patterns indicated that neither typical rotation pattern is sustainable.

3.3 Identification of best management practices

Out of the 6000 field management scenarios, three under the R_3 were finally identified as the BMP alternatives, which simultaneously satisfied the given constraints while yielding the comparably lowest NIPs (332−335 US$ ha^{-1} yr^{-1}) within the overlapping uncertain ranges with ε_s of −22 ± 16 US$ ha^{-1} yr^{-1} (Table 1). These BMP alternatives for the three-crop system recommended the following combination of field management practices including (i) the currently applied 6-year rotation cycle with three-year cotton monoculture rotated with three-year W-M, (ii) full incorporation of crop residues at harvest, (iii) the presently adopted crop cultivars and timing of sowing, fertilization (date, depth and splits), irrigation (date and times) and harvest, (iv) urea alone 18% lower rates (90 and 353 kg N ha^{-1} yr^{-1} for the cotton and W-M, respectively) than the conventional nitrogen fertilization, (v) sprinkling or flood-irrigation with ~23% less water (~77 mm per event) than the conventional flood-irrigation, and (vi) the conventional plough tillage (30 cm depth) following final cotton harvest but reduced tillage (rotary 5 cm depth) for the W-M. In comparison with the simulations driven by the baseline scenario (R_3 as the currently applied rotation pattern and its field management practices), the identified BMP alternatives could sustain the baseline crop yields while simultaneously enlarging the SOC stock by ≥ 4‰ and mitigating the NEGE, NH_3 volatilization, NO emission and NO_3^- leaching by ~7%, ~25%, ~2%, and ~43%, respectively, despite a slight increase (by ~5%) in the N_2O emission (Table 1).

4 Discussion

4.1 Model performance

The DNDC model has been widely applied in agricultural systems around the world. The version modified in this study showed good performance in simulating the soil environmental factors (soil temperature and moisture), crop yields, NEE, NH_3 volatilization, CH_4 uptake, emissions of N_2O and NO, and NO_3^- leaching for the investigated lands cultivated with cotton and W-M under different field management treatments. The satisfactory validations of both crop systems, especially for the constraint and decision variables at the annual scale, suggested that the modified DNDC95 could be applied to quantify the constraint and decision variables to determine the NIP for the cotton and W-M rotation system under various management practices.

The well-simulated soil environmental factors and crop yields provided a solid basis for further simulating the constraint and decision variables under any field management condition of the

three-crop rotation system. This is because the soil environmental factors are the key factors regulating the biogeochemical processes and crop yields are indicators of essential processes in plant nitrogen uptake (Chirinda et al., 2011; Kröbel et al., 2010). For the simulations of the N_2O and NO emissions, discrepancies in daily emissions generally occur in the simulations of DNDC or other current biogeochemical models due to the interactions among soil environmental factors and complex carbon- and nitrogen-related processes (e.g., Bell et al., 2012; Chirinda et al., 2011; Cui et al., 2014; Lehuger et al., 2011), which may ocassionally result in the significant time lags between the observations and simulations (e.g., Zhang et al., 2015). For the cotton in this study, the significant underestimation of daily NO fluxes in spring was solved to some extent through modifying the model version used by Cui et al. (2014). However, this improvement did not significantly affect the annual cumulative emissions, which were not mainly contributed by the spring fluxes (Liu et al., 2015). In fact, occasional time lags of one to a very few days for measured/simulated daily fluxes seldom lead to a significant modification for the seasonal/annual cumulative emissions of a nitrogenous gas. This is attributed to the control of the mass conservation law and the canceling effect of negative and positive daily errors. The modified algorithm improved the simulations of daily NEE fluxes, thus providing solid basis for yielding reliable annual/seasonal cumulative NEE quantities. According to the mass conservation law, the annual cumulative NEE can be involved in as one of the two additive items to estimate the annual ΔSOC of an annual crop system with retention/incorporation of full residues but without significant input/output of organic matter other than product removal at harvest. This approach may be used as an alternative algorithm in the modified model to simulate the annual ΔSOC of such a cropping system. In the present case study, the annual ΔSOC simulated by the modified model using this alternative approach were consistent with those simulated by the algorithm that quantifies the annual ΔSOC by summing up the annual carbon pool changes in the humus, microbial biomass and dissolvable organic compounds (Cui et al., 2014). The consistence was indicated by the |MRBs| of 20 ± 50% versus 37 ± 117% (95% CI) in comparison with the three observation-oriented estimates of annual ΔSOC (two for cotton and one for the W-M). Due to the marginally small sample size (n = 3), this preliminary result still requires confirmation in further study. The simulated NH_3 volatilizations from the cotton field accounted for 18−24% of the applied fertilizer nitrogen during the two year-round periods involved in the model

validation. These simulated nitrogen loss rates through NH_3 volatilization were comparable with the reported field measurements of 10−23% (Li et al., 2016).

The model validation in this study suggested that the satisfactory simulations of constraint and decision variables at the annual scale could provide a solid basis for BMP identification. Because of the limited annual observations of NH_3 volatilization, NO_3^- leaching and ΔSOC estimated from annually measured NEE, the insufficient validation still resulted in large uncertainties in the simulations of these three variables. Therefore, future studies are still required for further validation of the model performance using comprehensive observations covering these variables as well as the others, thus reducing the simulation errors of the constraint and decision variables so as to improve the screening precision of BMP alternatives.

4.2 Biogeochemical effects of rotation pattern and other management practices

The scenario analysis relying on model simulations in this study showed that environmental nitrogen contamination could be reduced while i) sustaining crop yields to protect food security, ii) achieving the 4‰ goal in soil carbon sequestration, and iii) decreasing the net ecosystem aggregate GHG emission to mitigate climate change. The reductions in environmental nitrogen contamination could be attributed to the better synchronization of crop nitrogen requirements and soil nitrogen availability through optimizing field management practices.

For cotton, a period of 5 consecutive years is usually applied as the longest cotton monoculture to stabilize its yields. Within this period, balanced elemental nutrients have been applied, and thus the negative effect of monoculture on cotton yields can be offset in practice (Han, 2010). In addition, the DNDC model assumes balanced nutrient supplies for any crops as well as optimum phytosanitary conditions, and thus the negative effects of monoculture are not taken into account (e.g., Li, 2017).

The simulated positive annual ΔSOC for the W-M cropping system were mainly attributed to the incorporation of the full aboveground residues (at rates of 5.1−7.0 Mg C ha^{-1} yr^{-1}), which in turn favored for carbon sequestration (Han et al., 2016). On the contrary, the simulations of annual ΔSOC for the cotton cropping system were negative. The SOC stock decreases resulted from (i) the more notable CO_2 emissions over the longer fallow season and (ii) the lower rates of fully incorporated residues (at rates of 2.5−3.1 Mg C ha^{-1} yr^{-1}) than those of the W-M (Liu et al., 2019). As a remarkable carbon sink, the W-M cropping system with the incorporation of the full crop residues even could

559 completely compensate for the SOC lost during the first cotton-planting year following the transition.
560 Thus, the simulated annual ΔSOC was generally positive during the first cotton cultivation year of a
561 three-crop rotation cycle. As a result, the R_0 (i.e., pure W-M continuously within each 6-year period)
562 acted as a net GHG sink since the positive ΔSOC could exceed the N_2O emission during the W-M
563 cultivation, whereas all the three-crop systems subject to R_1 to R_5 rotation patterns would function as
564 net GHG sources. The higher nitrogen application rate for the W-M than for the cotton resulted in more
565 reactive nitrogen remaining in the soil (Chen et al., 2014; Ju et al., 2009), thereby stimulating higher
566 emissions of N_2O and nitrogenous air pollutants in the trials with fewer cotton cultivation years.
567 Therefore, the rotation patterns of the cotton and W-M can be optimized to realize sustainable
568 intensification in terms of sustaining crop yields at a relatively high level, maximizing SOC increase
569 and minimizing negative impacts on the climate and environment.

570 Northern China, as the most important agricultural region, experienced an increase in crop yields
571 by a factor of 2.8 from 1980 to 2008. During this period, the application of mineral fertilizers increased
572 by a factor of 5.1. The rapid increase in fertilizer use has resulted in excessive nitrogen remaining in the
573 soil, posing potential risks for the environment (Chen et al., 2011; Zhang et al., 2017). To solve this
574 problem, a reduction in fertilizer application was proposed in several previous studies (e.g., Chen et al.,
575 2011, 2014; Liu et al., 2012). The results of the scenario analysis in this study indicated that further
576 reducing the farmer-optimized nitrogen doses by 18% could still sustain the crop yields while greatly
577 decreasing the release of nitrogenous pollutants.

578 In addition to fertilization, over-irrigation has also been ubiquitous in northern China for a long
579 time, and is threatening the water security of this region due to the sharply declining groundwater table
580 and water pollution (Gao et al., 2015; Ju et al., 2009). For this reason, only management options that
581 can reduce the amount of irrigation water should be recommended due to the severe shortage of water
582 resources in the region. In addition, adopting sprinkling irrigation instead of flood irrigation for an
583 equal amount of water showed positive effects on the crop yields, indicating improved irrigation
584 efficiency (Zhang et al., 2017). This result indicated that increasing the water-use efficiency through
585 the application of alternative irrigation techniques in coupling with reduced nitrogen doses could be a
586 pathway to sustain crop yields.

Reduced tillage practices have been promoted in China in the recent years. To facilitate the decomposition of the woody cotton residues and avoid outbreaks of diseases and pests induced by continuous implementation of reduced tillage or no-till, the tillage practices were only adjusted in the W-M fields, while currently applied deep tillage was maintained for the cotton when setting the tillage scenarios. The simulations showed that the reduced tillage or no-till practices could sustain the crop yields while reducing the NH_3 volatilization and NO_3^- leaching, which were consistent with the reports from experimental studies (e.g., Zhao et al., 2016).

As shown above, appropriate combinations of a rotation pattern and field management practices can satisfy the three given constraints while resulting in the lowest NIPs with overlapping uncertainties. However, direct observations in field experiments usually with very limited management treatments are far less sufficient for screening these appropriate combination alternatives. However, identifying the appropriate combination alternatives is one of the purposes of biogeochemical models, such as DNDC. In principle, a biogeochemical model that is validated with limited observations from field experiments, like the DNDC95 modified and used in this study, could be capable of fulfilling this task.

4.3 Evaluation of the best management practice

The scenario analysis in this study was effective for screening the BMP alternatives. The identified BMP alternatives could sustain the crop yields of the three-crop rotation system, increase the SOC stock annually at 4‰ for more, mitigate the NEGE, and reduce the NH_3 and NO emissions and NO_3^- leaching due to the enhanced resource use efficiency in response to the reduced nitrogen-fertilizer doses, irrigation water amounts and tillage depth for the W-M. Hence, the BMP alternatives could result in significantly reduced NIPs even compared to the currently applied field management practices that have been optimized by the local farmers. However, the identified BMP alternatives were based on the constraint and decision variables validated against only the observations at the single field site involved in this case study. In this regard, confirmation of these BMP alternatives at other sites of this region is still required in the future studies.

A biogeochemical model as an ideal tool for identifying the BMPs is reflected by near-zero ε_s for any constraint/decision variable or NIP. A small sample size of the observations used for validation of any constraint/decision variable would result in largely positive or negative ε_s (including large over- or under-estimations) for model simulations of the variable, likely account for the large ε_s of a NIP, and

thus lead to a lower precision in screening the BMP alternatives. Therefore, the applicability of the approach proposed in this study for identifying the BMPs is highly dependent upon the validations using observations with appropriate sample sizes for individual constraint and decision variables. In this study, the ε_s and ε_{input} for the simulated variables and NIPs of management scenarios were quantified. For the NIPs of the identified BMP alternatives, for instance, the ε_s and ε_{input} at relative magnitudes were 6.5 $\pm$4.9% and $\pm$3.3%, respectively, which were similar with those (9.1 $\pm$5.0% and $\pm$3.1%, respectively) of baseline scenario. According to these errors, the uncertain ranges of the NIPs for the three alternatives almost fully overlapped with each other while they were all beyond the uncertain range of the NIP for the baseline scenario. This implicated that the approach proposed in this study could be applicable for identifying the BMPs of the three-crop rotation system. Nevertheless, the ε_s uncertain range of one times SD still fully diverged negatively from zero, due to the marginally small sample sizes of available ΔSOC, NH_3 volatilization and NO_3^- leaching observations that led to insufficient validations for these variables. Especially, the model underestimations of NO_3^- leaching (with an adjusting factor of 1.42 and error factors of -29 ± 4%) overwhelmingly dominated the diverged ε_s of the NIPs, which were comparable or larger than the ε_{input} values. Relying on the few field observations, one was still not able to judge whether there are insufficiencies in the scientific structures or inappropriate parameters in the model to dominate the large ε_s for these variables. Therefore, multiple comprehensive field observations with appropriate sample sizes to fully cover all the relevant variables are as substantially necessary as an advanced biogeochemical model with multiple functions in order to address the best management issue of a multi-crop rotation system to achieve multiple benefits.

The DNDC model has been established by following the mass conservation law. In other words, this model can accurately reflect the mass balance of the carbon or nitrogen budgets for the simulated soil layer (0−50 cm depth). This principle implies that only one nitrogen budget item could be omitted for model validation. This item is usually soil nitrogen loss through the production of dinitrogen gas (N_2), mainly by denitrification, which is very difficult to measure *in situ* (e.g., Wang et al., 2013; Zhang et al., 2019). For both crop cropping systems, however, the nitrogen lost through this pathway could be almost fully inhibited in the topsoil, wherein the soil moisture contents were often lower than 60%

644 WFPS (Linn and Doran, 1984; Liu et al., 2011, 2014). For instance, the N_2 emission likely accounts for
645 approximately 1.6% of the urea applied in a winter wheat season (Zhang et al., 2019), which is at a
646 negligibly low level for the nitrogen balance.

647 Regarding the identification of the BMPs, the approach proposed and applied in this case study
648 only includes the biogeochemical effects of management on the constraint/decision variables. This
649 approach currently excludes other factors, such as those related to the costs of the management
650 practices, thereby likely resulting in uncertainties in the screened BMP alternatives. Despite some
651 deficiencies, this approach can be easily and automatically implemented as long as the simulations for
652 all constraint and decision variables can be validated using comprehensive observations, implicating its
653 potential applicability for more comprehensive situations. Adding the missing factors is one of the
654 future research tasks to further improve this approach.

655 **5 Conclusions**

656 To address the challenging issue for optimizing multi-crop system management to simultaneously
657 achieve multiple benefits, a biogeochemical model-based approach for identifying the best
658 management practices (BMPs) was proposed and tested in this site-scale case study. A three-crop
659 system widely distributed in northern China, which grew cotton in rotation with winter wheat and
660 summer maize (W-M), was investigated. The BMPs were referred to the management alternatives with
661 the lowest negative impact potentials (NIPs), falling overlapping uncertain ranges, among the scenarios
662 satisfying a set of constraints. The NIP of a scenario was defined as the linear function of five decision
663 variables, including the net ecosystem aggregate greenhouse gas emission (NEGE), ammonia (NH_3)
664 volatilization, nitric oxide (NO) release, emission of nitrous oxide (N_2O) as an ozone layer depletion
665 matter, and nitrate leaching. This study used three variables, i.e., crop yield, annual change in SOC
666 stock (ΔSOC), and NEGE, to specify the applied constraints that were stable/increased crop yields,
667 annual ΔSOC by 4‰ or more, and reduced annual NEGE by at least 5% in comparison with those of
668 the baseline scenario (as the currently applied practices in this study). The constraint and decision
669 variables to determine the NIP of each scenario were provided by the simulation of
670 DeNitrification-DeComposition version 95 model (DNDC95) modified in this study. Due to the
671 unsatisfactory performance of the model in daily simulations of NO emission and net ecosystem
672 exchange of carbon dioxide (NEE), the model was modified to include a new parameterization of soil

moisture effects on the NO production during nitrification and replacement of the original calculation approach for NEE with an algorithm based on gross primary production. For the concerned variables with available measurements in two adjacent lands at the selected field site, the modified model showed statistically meaningful consistence between simulations and observations. Using the systematic errors obtained from the model validation to determine the simulation uncertainties of the concerned variables for each scenario and that of its NIP, the modified model simulations driven by 6000 management scenarios automatically identified three BMP alternatives. These BMP alternatives follow the current adopted rotation pattern (3 consecutive years of cotton rotated with 3 continuous years of W-M) applied with 18% less fertilizer nitrogen and ~23% less irrigation water through sprinkling or flooding and reduced depth of tillage for the W-M even in comparison with the current applied farmer-optimized management practices. This case study demonstrated the practicability of the model-based approach and implicated its potential applicability for optimizing the field management of multi-crop system to simultaneously achieve multiple United Nations Sustainable Development Goals. It also emphasized the need to make comprehensive observations that fully cover the constraint and decision variables, other related factors as well as all the crops and management practices in question to facilitate effective BMP screening through virtual experiments using a biogeochemical model, such as DNDC. In the future study to identify the BMPs specifically for the three-crop rotation system at the regional scale, it is still necessary for a 6-year model validation that includes a rotation of all three commodity crops as well as all studied management practices in question.

Data availability

All the model output for producing the figures can be obtained from the supplementary materials and all the observed data sets used in this study can be available from the co-authors.

Author contributions

X, Zheng, C, Liu and J, Zhu contributed to develop the idea and enhance the science of this study. W, Zhang proposed a new evaluation factor – negative impact potential, designed and implemented the model simulations and virtual experiments and prepared the manuscript with contributions from all co-authors. C, Liu, K, Wang, R, Wang and Z, Yao contributed to obtain the field measured data. F, Cui and S, Li contributed to the model validation for the winter wheat-summer maize cropping system.

Competing interests

The authors declare that they have no conflict of interest.

Acknowledgement

This study was jointly supported by the National Key R&D Program of China (2016YFA0602303) and the National Natural Science Foundation of China (41603075, 41761144054).

706 **References**

707 Beheydt, D., Boeckx, P., Sleutel, S., Li, C., Vancleemput, O.: Validation of DNDC for 22 long-term
708 N_2O field emission measurements. Atmos. Environ., 41, 6196-6211, 2007.

709 Chen, X., Cui, Z., Vitousek, P., Cassman, K., Matson, P., Bai, J., Meng, Q., Hou, P., Yue, S., Romheld,
710 V., and Zhang, F.: Integrated soil-crop system management for food security, Proc. Natl. Acad. Sci.
711 U. S. A., 108, 6399–6404, 1101419108, 2011.

712 Chen, X., Cui, Z., Fan, M., Vitousek, P., Zhao, M., Ma, W., Wang, Z., Zhang, W., Yan, X., Yang, J.,
713 Deng, X., Gao, Q., Zhang, Q., Guo, S., Ren, J., Li, S., Ye, Y., Wang, Z., Huang, J., Tang, Q., Sun,
714 Y., Peng, X., Zhang, J., He, M., Zhu, Y., Xue, J., Wang, G., Wu, L., An, N., Wu, L., Ma, L., Zhang,
715 W., and Zhang, F.: Producing more grain with lower environmental costs, Nature, 514, 486–489.
716 2014.

717 China Statistical Yearbook: Agriculture, Complied by National Bureau of Statistics of China, China
718 Statistics Press, Beijing, Published online, http://www.stats.gov.cn/tjsj/ndsj/2017/indexch.htm,
719 2017.

720 Chirinda, N., Kracher, D., Lægdsmand, M., Porter, J.R., Olesen, J.E., Petersen, B.M., Doltra, J., Kiese,
721 R., and Butterbach-Bahl, K.: Simulating soil N_2O emissions and heterotrophic CO_2 respiration in
722 arable systems using FASSET and MoBiLE-DNDC, Plant Soil, 343, 139–160, 2011.

723 Collins, A.L., Zhang, Y.S., Winter, M., Inman, A., Jones, J.I., Johnes, P.J., Cleasby, W., Vrain, E.,
724 Lovett, A., and Noble, L.: Tackling agricultural diffuse pollution: What might uptake of
725 farmer-preferred measures deliver for emissions to water and air? Sci. Total Environ., 547, 269–
726 281, 2016.

727 Congreves, K.A., Grant, B.B., Dutta, B., Smith, W.N., Chantigny, M.H., Rochette, and Desjardins, R.L.:
728 Prediction ammonia volatilization after field application of swine slurry: DNDC model
729 development, Agr. Ecosyst. Environ., 219, 179–189, 2016.

730 Cui, F., Zheng, X., Liu, C., Wang, K., Zhou, Z., and Deng, J.: Assessing biogeochemical effects and
731 best management practice for a wheat-maize cropping system using the DNDC model,
732 Biogeosciences, 11, 91–107, 2014.

733 Delgrosso, S., Mosier, A., Parton, W., and Ojima, D.: DAYCENT model analysis of past and
734 contemporary soil NO and net greenhouse gas flux for major crops in the USA, Soil Till. Res., 83,

9–24, 2005.

Ding, W., Meng, L., Yin, Y., Cai, Z., and Zheng, X.: CO_2 emission in an intensively cultivated loam as affected by long-term application of organic manure and nitrogen fertilizer, Soil Biol. Biochem., 39, 669–679, 2007.

Dubache, G., Li, S., Zheng, X., Zhang, W., and Deng, J.: Modeling ammonia volatilization following urea application to winter cereal fields in the United Kingdom by improving a biogeochemical model, Sci. Total Environ., 660, 1403–1418, 2019.

Galloway, J.N., Dentenerd, F.J., Capone, D.G., Boyer, E.W., Howarth, R.W., Seitzinger, S.P., Asner, G.P., Cleveland, C.C., Green, P.A., Holland, E.A., Karl, D.M., Michaels, A.F., Porter, J.H., Townsend, A.R., and Vorosmarty, C.J.: Nitrogen Cycles: past, present, and future, Biogeochemistry, 70, 153–226, 2004.

Gao, B., Ju, X., Meng, Q., Cui, Z., Christie, P., Chen, X., and Zhang, F.: The impact of alternative cropping systems on global warming potential, grain yield and groundwater use, Agr. Ecosyst. Environ., 203, 46–54, 2015.

Garnett, T., Appleby, M.C., Balmford, A., Bateman, I.J., Benton, T.G., Bloomer, P., Burlingame, B., Dawkins, M., Dolan, L., and Fraser, D.: Sustainable intensification in agriculture: premises and policies, Science, 341, 33–34, 2013.

Haas, E., Klatt, S., Fröhlich, A., Kraft, P., Werner, C., Kiese, R., Grote, R., Breuer, L., and Butterbach-Bahl, K.: LandscapeDNDC: a process model for simulation of biosphere-atmosphere-hydrosphere exchange processes at site and regional scale, Landscape Ecol, 28, 615–636, 2012.

Han, C.: Temporal and spatial variation of soil nutrients of long-term monocultural cotton field and soil sustainable utilization in Xinjiang (Dissertation), Shihezi University, 2010.

Han, P., Zhang, W., Wang, G., Sun, W., and Huang, Y.: Changes in soil organic carbon in croplands subjected to fertilizer management: a global meta-analysis, Sci. Rep., 6, 27199, 2016.

Intergovernmental Panel on Climate Change (IPCC): Climate Change 2013: The Physical Science Basis, Contribution of Working Group I to the Fifth Assessment Report of the Intergovernmental Panel on Climate Change (eds. Stocker TF, Qin D, Plattner G-K, et al.), Cambridge University

763 Press, Cambridge, United Kingdom and New York, NY, USA, 2013.
764 Jiang, Z.: Analysis on the establishment conditions of the square sum decomposition formular of
765 regression model, J. Industr. Techn. Econ., 29(4), 116–119, 2010 (in Chinese).
766 Ju, X., Xing, G., Chen, X., Zhang, S., Zhang, L., Liu, X., Cui, Z., Yin, B., Christie, P., Zhu, Z., and
767 Zhang, F.: Reducing environmental risk by improving N mannagement in intensive Chinese
768 agricultural systems, Proc. Natl. Acad. Sci. U. S. A., 106, 3041–3046, 2009.
769 Kröbel, R., Sun, Q., Ingwersen, J., Chen, X., Zhang, F., Müller, T., and Römheld, V.: Modelling water
770 dynamics with DNDC and DAISY in a soil of the North China Plain: A comparative study,
771 Environ. Modell. Softw., 25, 583–601, 2010.
772 Lehuger, S., Gabrielle, B., Laville, P., Lamboni, M., Loubet, B., Cellier, P.: Predicting and mitigating
773 the net greenhouse gas emissions of crop rotations in Western Europe. Agr. Forest Meteorol., 151,
774 1654-1671, 2011.
775 Li, C.: Modeling trace gas emissions from agricultural ecosystems, Nutr. Cycl. Agroecosyst., 58, 259–
776 276, 2000.
777 Li, C.: Quantifying greenhouse gas emissions from soils: Scientific basis and modeling approach, J.
778 Soil Sci. Plant Nut., 53, 344–352, 2007.
779 Li, C.: Biogeochemistry: Scientific Fundamentals and Modelling Approach, Tsinghua University Press,
780 Beijing, 2016 (in Chinese).
781 Li, C., Frolking, S., and Frolking, T.A.: A model of nitrous oxide evolution from soil driven by rainfall
782 events: 1. Model Structure and Sensitivity, J. Geophys. Res., 97, 9759–9776, 1992.
783 Li, H., Wang, L., Li, J., Gao, M., Zhang, J., Zhang, J., Qiu, J., Deng, J., Li, C., and Frolking, S.: The
784 development of China-DNDC and review of its applications for sustaining Chinese agriculture,
785 Ecol. Model., 348, 1–13, 2017.
786 Li, M., Liang, W., Zheng, X., Yang, Z., Zheng, P., Chen, Y., and Chen, D.: Characteristics of NO
787 emission from typical saline soil of southern Shanxi cotton land, Climatic Environ. Res., 14, 318–
788 328, 2009 (in Chinese).
789 Li, Q., Liao, N., Zhang, N., Zhou, G., Zhang, W., Wei, X., Ye, J., and Hou, Z.: Effects of cotton
790 (Gossypium hirsutum L.) straw and its biochar application on NH_3 volatilization and N use

efficiency in a drip-irrigated cotton field, J. Soil Sci. Plant Nut., 62, 534–544, 2016.

Li, S., Zheng, X., Zhang, W., Han, S., Deng, J., Wang, K., Wang, R., Yao, Z., and Liu, C.: Modeling ammonia volatilization folllowing the application of synthetic fertilizers to cultivated uplands with calcareous soils using an improved DNDC biogeochemstry model, Sci. Total Environ., 660, 931–946, 2019.

Linn, D.M. and Doran, J.W.: Effect of water-filled pore space on carbon dioxide and nitrous oxide production in tilled and nontilled soils, Soil Sci. Soc. Am. J., 48, 1267–1272, 1984.

Liu, C., Zheng, X., Zhou, Z., Han, S., Wang, Y., Wang, K., Liang, W., Li, M., Chen, D., and Yang, Z.: Nitrous oxide and nitric oxide emissions from an irrigated cotton field in Northern China, Plant Soil, 332, 123–134, 2010.

Liu, C., Wang, K., Meng, S., Zheng, X., Zhou, Z., Han, S., Chen, D., and Yang, Z.: Effects of irrigation, fertilization and crop straw management on nitrous oxide and nitric oxide emissions from a wheat-maize rotation field in northern China, Agr. Ecosyst. Environ., 140, 226–233, 2011.

Liu, C., Wang, K., and Zheng, X.: Responses of N_2O and CH_4 fluxes to fertilizer nitrogen addition rates in an irrigated wheat-maize cropping system in northern China, Biogeosciences, 9, 839–850, 2012.

Liu, C., Yao, Z., Wang, K., and Zheng, X.: Three-year measurements of nitrous oxide emissions from cotton and wheat-maize rotational cropping systems, Atmos. Environ., 96, 201–208, 2014.

Liu, C., Yao, Z., Wang, K., and Zheng, X.: Effects of increasing fertilization rates on nitric oxide emission and nitrogen use efficiency in low carbon calcareous soil, Agr. Ecosyst. Environ., 203, 83–92, 2015.

Liu, C., Yao, Z., Wang, K., Zheng, X., and Li, B.: Net ecosystem carbon and greenhouse gas budgets in fiber and cereal cropping systems, Sci. Total Environ., 647, 895–904, 2019.

Lv, J., Liu, X., Liu, H., Wang, X., Li, K., Tian, C., and Christie, P.: Greenhouse gas intensity and net annual global warming potential of cotton cropping systems in an extremely arid region, Nutr. Cycl. Agroecosyst., 98, 15–26, 2014.

Moriasi, D.N., Arnold, J.G., Van Liew, M.W., Bingner, R.L., Harmel, R.D., and Veith, T.L.: Model evaluation guidelines for systematic quantification of accuracy in watershed simulation, T. Am.

819 Soc. Agr. Biol. Eng., 50, 885–900, 2007.
820 Nash, J.E. and Sutcliffe, J.V.: River flow forecasting through conceptual models: part I- a discussion of
821 principles, J. Hydrol., 10, 282–290, 1970.
822 Palosuo, T., Foereid, B., Svensson, M., Shurpali, N., Lehtonen, A., Herbst, M., Linkosalo, T., Ortiz, C.,
823 Rampazzo Todorovic, G., Marcinkonis, S., Li, C., and Jandl, R.: A multi-model comparison of soil
824 carbon assessment of a coniferous forest stand, Environ. Modell. Softw., 35, 38–49, 2012.
825 Tong, H., Zheng, X., Wang, R., Zhou, Z., Yue, J., Liu, C., Li, M., Liang, W., and Dong, H.: A
826 preliminary study of measurement of NH_3 volatilization from cropland using Qusi-dynamic
827 chamber, Clim. Environ. Res., 14(4), 373–382, 2009 (in Chinese).
828 Wang, E., Yu, Q., Wu, D., and Xia, J.: Climate, agricultural production and hydrological balance in the
829 North China Plain, Int. J. Climatol., 28, 1959–1970, 2008.
830 Wang, K., Liu, C., Zheng, X., Pihlatie, M., Li, B., Haapanala, S., Vesala, T., Liu, H., Wang, Y., Liu, G.,
831 and Hu, F.: Comparison between eddy covariance and automatic chamber techniques for
832 measuring net ecosystem exchaange of carbon dioxide in cotton and wheat fields, Biogeosciences,
833 10, 6865–6877, 2013a.
834 Wang, K., Zheng, X., Pihlatie, M., Vesala, T., Liu, C., Haapanala, S., Mammarella, I., Rannik, Ü., and
835 Liu, H.: Comparison between static chamber and tunable diode laser-based eddy covariance
836 techniques for measuring nitrous oxide fluxes from a cotton field, Agr. Forest. Meteorl., 171–172,
837 9–19, 2013b.
838 Wang, R., Feng, Q., Liao, T., Zheng, X., Butterbach-Bahl, K., Zhang, W., and Jin, C.: Effects of nitrate
839 concentration on the denitrification potential of a calcic cambisol and its fractions of N_2, N_2O and
840 NO, Plant Soil, 363, 175–189, 2013.
841 Willmott, C.J. and Matsuurra, K.: Advantages of the mean aboslute error (MAE) over the root mean
842 square error (RMSE) in assessing average model performance, Clim. Res., 30, 79–82, 2005.
843 Xu, Q., Li, Z., Hu, K., and Li, B.: Optimal management of water and nitrogen for farmland in North
844 China Plain based on osculating value method and WHCNS model, Transaction of the Chinese
845 Society of Agricultural Engineering, 33, 152–158, 2017 (in Chinese).
846 Yang, Z., Turner, D., Zhang, J., Wang, Y., Chen, M., Zhang, Q., Denmead, Q., Che, D., and Freney, J.:

Loss of nitrogen by ammonia volatilzation and denitrification after application of urea to maize in Shanxi Province, China, Soil Res., 49, 462–469, 2011.

Zhang, W., Liu, C., Zheng, X., Zhou, Z., Cui, F., Zhu, B., Haas, E., Klatt, S., Butterbach-Bahl, K., and Kiese, R.: Comparison of the DNDC, LandscapeDNDC and IAP-N-GAS models for simulating nitrous oxide and nitric oxide emissions from the winter wheat-summer maize rotation system, Agric. Syst., 140, 1–10, 2015.

Zhang, W., Li, Y., Zhu, B., Zheng, X., Liu, C., Tang, J., Su, F., Zhang, C., Ju, X., and Deng, J.: A process-oriented hydro-biogeochemical model enabling simulation of gaseous carbon and nitrogen emissions and hydrologic nitrogen losses from a subtropical catchment, Sci. Total Environ., 616–617, 305–317, 2018.

Zhang, X., Bol, R., Rahn, C., Xiao, G., Meng, F., and Wu, W.: Agricultural sustainable intensification improved nitrogen use efficiency and maintained high crop yield during 1980−2014 in Northern China, Sci. Total Environ., 596-597, 61–68, 2017.

Zhao, X., Liu, S.L., Pu, C., Zhang, X.Q., Xue, J.F., Zhang, R., Wang, Y.Q., Lal, R., Zhang, H.L., and Chen, F.: Methane and nitrous oxide emissions under no-till farming in China: a meta-analysis, Global Change Biol., 22, 1372–1384, 2016.

Zhang, Y., Wang, R., Pan, Z., Liu, Y., Zheng, X., Ju, X., Zhang, C., Butterbach-Bahl, K., Huang, B.: Fertlizer nitrogen loss via N_2 emission from calcareous soil following basal urea application of winter wheat, Atmos, Oceanic Sci. Lett., 12, 91–97, 2019.

Zheng, X., Xie, B., Liu, C., Zhou, Z., Yao, Z., Wang, Y., Wang, Y.,Yang, L., Zhu, J., Huang, Y., and Butterbach-Bahl, K.: Quantifying net ecosystem carbon dioxide exchange of a short-plant cropland with intermittent chamber measurements, Global Biogeochem. Cycl., 22, GB3031.

Table and figure captions

Table 1 Simulated constraint and decision variables and negative impact potentials (NIPs) for the baseline (the conventionally applied practices) and the alternatives of the best management practices.

Figure 1: Observed and simulated daily mean soil (5 cm) temperature, soil (0−6 cm) moisture, daily net ecosystem exchanges of carbon dioxide (NEE) in cotton field and winter wheat-summer maize fields, and daily fluxes of methane (CH_4), nitrous oxide (N_2O) and nitric oxide (NO) from cotton field. The solid- and dashed-line arrows indicate the dates of fertilization and irrigation, respectively. The measurement errors were not shown in panels a−e for figure clarity. The vertical bar for each observation in panels f−h indicates double standard deviations to represent the uncertain at the 95% confidence interval. The legends in panel c apply for all subfigures.

Figure 2: Comparison between observations and simulations of crop yields, annual/seasonal cumulative NEE and NEGE, and annual/seasonal ΔSOC, and annual cumulative fluxes of methane (CH_4) uptake, nitrous oxide (N_2O) and nitric oxide (NO), and cumulative fluxes of ammonia (NH_3). Yield, seed yield of cotton (open cycle) and grain yield of winter wheat (solid cycle) and summer maize (solid diamond). NEE, net ecosystem exchanges of carbon dioxide. NEGE, net ecosystem aggregate greenhouse gas emission. ΔSOC, change in soil organic carbon stock. Given NEE, NEGE and ΔSOC are annual for cotton and seasonal for wheat and maize. The observed ΔSOC was given as the opposite of NEE plus yield in carbon mass quantity for the cropping system with incorporation of full residues whereas each ΔSOC simulation was the sum of simulated changes in carbon stocks of soil humus, microbial biomass and dissolvable organic compounds. Simulations were resulted from the modified model. Given slope errors of the zero-intercept linear regressions are double standard deviations to represent the 95% confidence interval. Vertical bars indicate standard deviation of three or four spatial replicates, with exception for NEE. Given errors of NEE were adapted from the coefficient of variation on average (25%) reported by Wang et al. (2013b). DM, dry matter. CO_2eq, carbon dioxide equivalent. The 100-year global warming potentials of 34 for CH_4 and 298 for N_2O (IPCC, 2013) were used to quantify NEGE in CO_2eq quantity.

Figure 3: Simulated cumulative crop yields, changes in soil organic carbon (ΔSOC), methane (CH_4), nitrous oxide (N_2O) releases, net ecosystem aggregate greenhouse gas emission (NEGE), ammonia (NH_3) volatilization, nitric oxide (NO) emission and nitrate leaching (NL) of individual rotation

patterns (with a 6-year rotation cycle) over a 18-year period. R_0, R_1, ..., R_5 represents the rotation pattern with the cotton cultivated consecutively for 0, 1, ..., 5 year(s), respectively, within each 6-year rotation cycle. The legends in panel e apply for all subfigures. Given simulations resulted from the modified model driven by the currently applied field management practices (i.e., the baseline field management scenario) and observed means of input soil properties.

Figure 4: Simulated effects of various rotation patterns between cotton and winter wheat-summer maize cropping system with a 6-year cycle on decision variables and negative impact potential (NIP). The subscript of R_0, R_1, ..., R_5 are referred to the number of consecutive years for cotton cultivation. The y-axis units are Mg C ha^{-1} yr^{-1} for the opposite of mean annual increase in soil organic carbon stock ($-\Delta$SOC), kg C ha^{-1} yr^{-1} for methane (CH_4) emission, kg N ha^{-1} yr^{-1} for fluxes of nitrous oxide (N_2O), ammonia (NH_3) and nitrous oxide (NO), and nitrate leaching (NL), Mg CO_2eq ha^{-1} yr^{-1} for net ecosystem aggregate greenhouse gas emission (NEGE), and US$ ha^{-1} yr^{-1} for NIP. The CO_2eq was based on the 100-year global warming potentials, i.e., 34 for CH_4 and 298 for N_2O (IPCC, 2013). The NIP was calculated using Eq. 7 presented in the text. The vertical bar within the open cycle of each datum point indicates the absolute uncertainty (1 standard deviation) induced by input uncertainties of key soil properties. Each unfilled column indicates the absolute total uncertainty of the simulation, with its vertical bar representing its random uncertainty (1 standard deviation).

Table 1 Simulated constraint and decision variables and negative impact potentials (NIPs) for the baseline (the conventionally applied practices) and the alternatives of the best management practices.

Scenarios					R	Constraint variable											Decision variable						NIP	
						Yield					ΔSOC			NEGE										
	N	IA	IM	T		Sim_{cotton}	Sim_{wheat}	Sim_{maize}	ε_s	ε_{input}	Sim	ε_s	ε_{input}	Sim	ε_s	ε_{input}	CH_4	N_2O	NH_3	NO	NL	Sim	ε_s	ε_{input}
BAS	110/430	100	IF	20	R_3	3.5	4.8	6.8	0.15 (0.08)	0.04	0.14	0.03 (0.02)	0.02	1.06	0.22 (0.15)	0.18	−1.88	3.55	57	1.60	58	453	−41 (22)	14
BMP_1	90/353	79	IS	5	R_3	3.6	4.8	6.8	0.15 (0.08)	0.03	0.19	0.04 (0.03)	0.02	0.98	0.20 (0.14)	0.19	−1.81	3.71	43	1.57	33	332	−22 (16)	11
BMP_2	90/353	76	IS	5	R_3	3.6	4.8	6.8	0.15 (0.08)	0.03	0.18	0.04 (0.03)	0.02	0.98	0.20 (0.14)	0.20	−1.81	3.71	43	1.57	33	333	−22 (16)	11
BMP_3	90/353	76	IF	5	R_3	3.5	4.8	6.8	0.15 (0.08)	0.03	0.18	0.04 (0.03)	0.01	1.00	0.21 (0.15)	0.20	−1.83	3.76	44	1.56	33	335	−22 (16)	11

[a] BAS, the baseline. BMP, different best management alternatives denoted by subscript numbers. N, nitrogen fertilizer dose (kg N ha^{-1} yr^{-1}) of cotton/wheat-maize (W-M). IA, irrigation water amount (mm per event). IM, irrigation method. IF, flood-irrigation. IS, sprinkling irrigation. T, tillage depth (cm). R, rotation pattern. R_3, rotation pattern with 3 consecutive years of cotton rotated with 3 continuous years of W-M. Yield, seed (cotton) or grain (W-M) yield (Mg ha^{-1} in dry matter). Sim, annual quantity simulation. ε_s, the absolute total simulation error (i.e., the systematic error) of the annual quantity simulation, with its error (1 standard deviation) representing the random uncertain magnitude. ε_{input}, the random model simulation error (1 standard deviation) due to input uncertainties of the key soil properties including clay fraction, bulk density, pH and soil organic carbon content. ΔSOC, annual change in soil organic carbon stock in the 0−50 cm (Mg C ha^{-1} yr^{-1}). NEGE, net ecosystem aggregate greenhouse gas emission in carbon dioxide equivalent (Mg CO_2eq ha^{-1} yr^{-1}). CH_4, methane emission (kg C ha^{-1} yr^{-1}). N_2O, NH_3, NO and NL, emission of nitrous oxide, ammonia, and nitric oxide, and nitrate leaching, respectively (kg N ha^{-1} yr^{-1}). The CO_2eq was based on the 100-year global warming potentials of 34 for CH_4 and 298 for N_2O (IPCC, 2013). NIP, negative impact potential (US$ ha^{-1} yr^{-1}). Given simulations are the averages of 18 consecutive years.

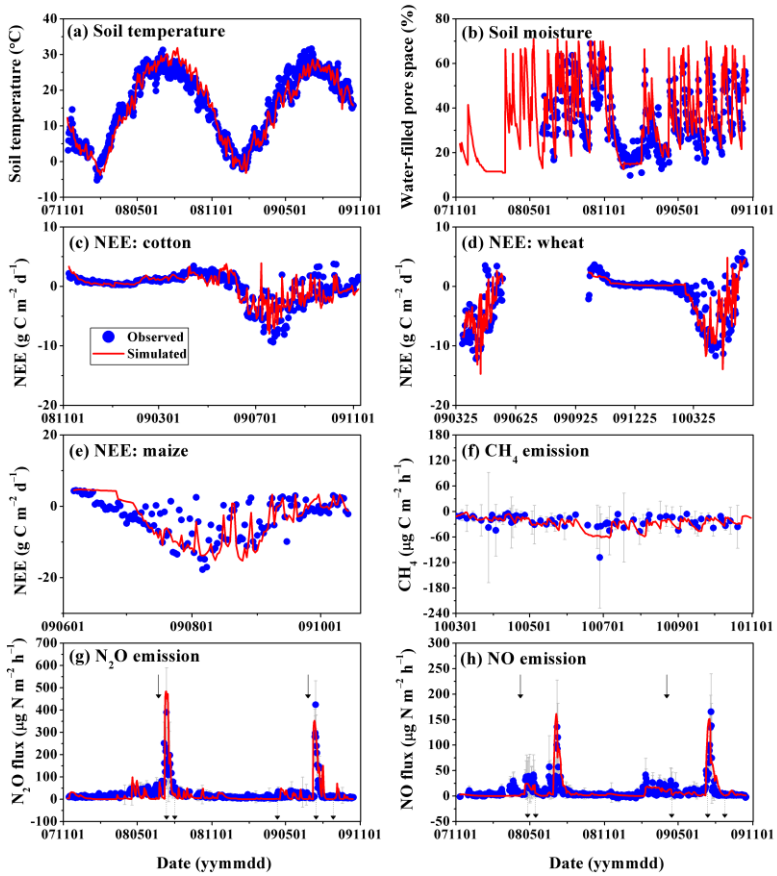

925

926 **Figure 1: Observed and simulated daily mean soil (5 cm) temperature, soil (0−6 cm) moisture, daily net**
927 **ecosystem exchanges of carbon dioxide (NEE) in cotton field and winter wheat-summer maize fields, and**
928 **daily fluxes of methane (CH_4), nitrous oxide (N_2O) and nitric oxide (NO) from cotton field. The solid- and**
929 **dashed-line arrows indicate the dates of fertilization and irrigation, respectively. The measurement errors**
930 **were not shown in panels a−e for figure clarity. The vertical bar for each observation in panels f−h indicates**
931 **double standard deviations to represent the uncertain at the 95% confidence interval. The legends in panel c**
932 **apply for all subfigures.**

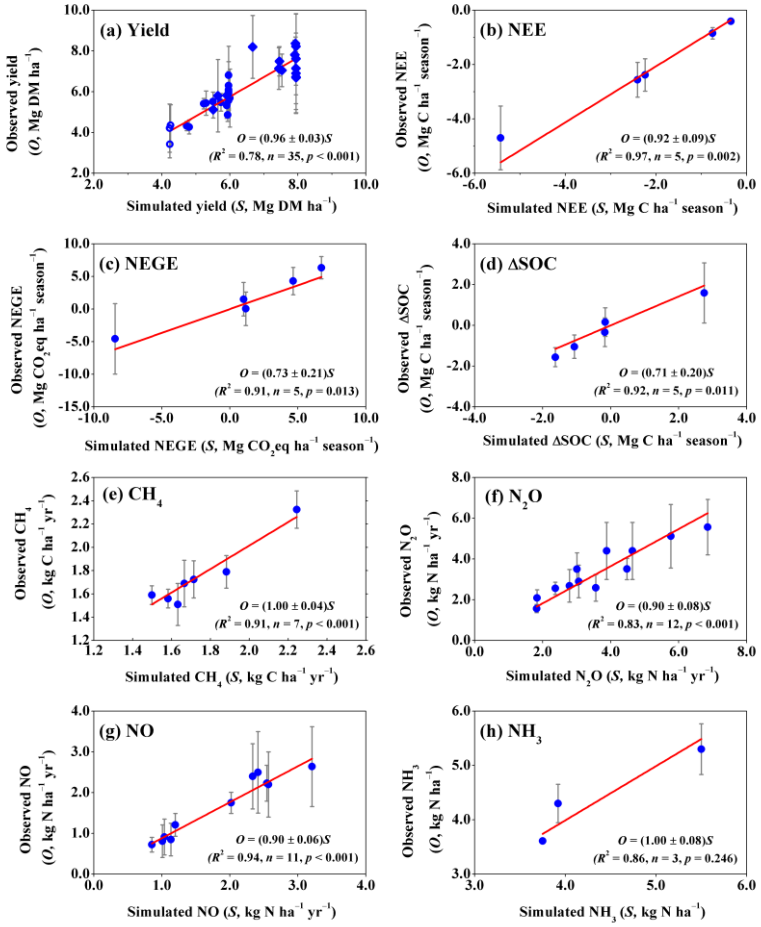

933

934 **Figure 2: Comparison between observations and simulations of crop yields, annual/seasonal cumulative**
935 **NEE and NEGE, and annual/seasonal ΔSOC, and annual cumulative fluxes of methane (CH_4) uptake,**
936 **nitrous oxide (N_2O) and nitric oxide (NO), and cumulative fluxes of ammonia (NH_3). Yield, seed yield of**
937 **cotton (open cycle) and grain yield of winter wheat (solid cycle) and summer maize (solid diamond). NEE,**
938 **net ecosystem exchanges of carbon dioxide. NEGE, net ecosystem aggregate greenhouse gas emission. ΔSOC,**
939 **change in soil organic carbon stock. Given NEE, NEGE and ΔSOC are annual for cotton and seasonal for**
940 **wheat and maize. The observed ΔSOC was given as the opposite of NEE plus yield in carbon mass quantity**
941 **for the cropping system with incorporation of full residues whereas each ΔSOC simulation was the sum of**
942 **simulated changes in carbon stocks of soil humus, microbial biomass and dissolvable organic compounds.**
943 **Simulations were resulted from the modified model. Given slope errors of the zero-intercept linear**
944 **regressions are double standard deviations to represent the 95% confidence interval. Vertical bars indicate**
945 **standard deviation of three or four spatial replicates, with exception for NEE. Given errors of NEE were**
946 **adapted from the coefficient of variation on average (25%) reported by Wang et al. (2013b). DM, dry matter.**
947 **CO_2eq, carbon dioxide equivalent. The 100-year global warming potentials of 34 for CH_4 and 298 for N_2O**
948 **(IPCC, 2013) were used to quantify NEGE in CO_2eq quantity.**

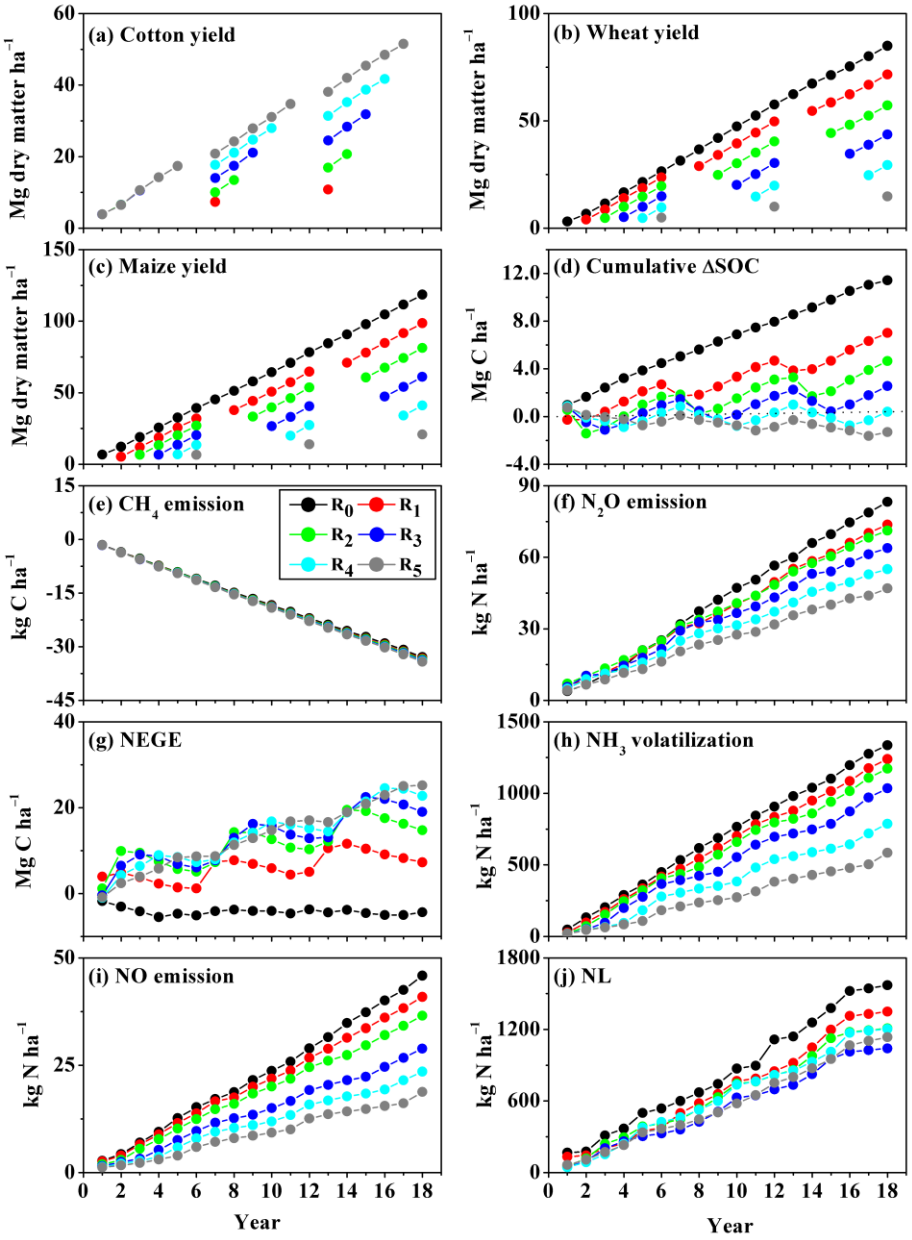

Figure 3: Simulated cumulative crop yields, changes in soil organic carbon (ΔSOC), methane (CH_4), nitrous oxide (N_2O) releases, net ecosystem aggregate greenhouse gas emission (NEGE), ammonia (NH_3) volatilization, nitric oxide (NO) emission and nitrate leaching (NL) of individual rotation patterns (with a 6-year rotation cycle) over a 18-year period. R_0, R_1, ..., R_5 represents the rotation pattern with the cotton cultivated consecutively for 0, 1, ..., 5 year(s), respectively, within each 6-year rotation cycle. The legends in panel e apply for all subfigures. Given simulations resulted from the modified model driven by the currently applied field management practices (i.e., the baseline field management scenario) and observed means of input soil properties.

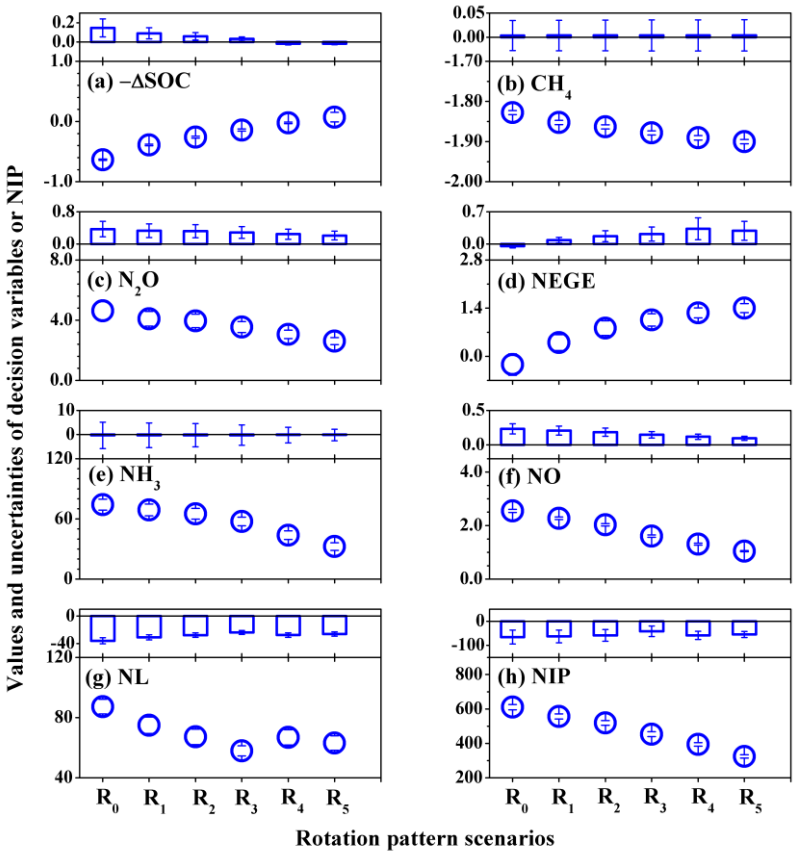

Figure 4: Simulated effects of various rotation patterns between cotton and winter wheat-summer maize cropping system with a 6-year cycle on decision variables and negative impact potential (NIP). The subscript of R_0, R_1, ..., R_5 are referred to the number of consecutive years for cotton cultivation. The y-axis units are Mg C ha^{-1} yr^{-1} for the opposite of mean annual increase in soil organic carbon stock (−ΔSOC), kg C ha^{-1} yr^{-1} for methane (CH_4) emission, kg N ha^{-1} yr^{-1} for fluxes of nitrous oxide (N_2O), ammonia (NH_3) and nitrous oxide (NO), and nitrate leaching (NL), Mg CO_2eq ha^{-1} yr^{-1} for net ecosystem aggregate greenhouse gas emission (NEGE), and US$ ha^{-1} yr^{-1} for NIP. The CO_2eq was based on the 100-year global warming potentials, i.e., 34 for CH_4 and 298 for N_2O (IPCC, 2013). The NIP was calculated using Eq. 7 presented in the text. The vertical bar within the open cycle of each datum point indicates the absolute uncertainty (1 standard deviation) induced by input uncertainties of key soil properties. Each unfilled column indicates the absolute total uncertainty of the simulation, with its vertical bar representing its random uncertainty (1 standard deviation).